Establishment of the light-absorption ratio variation approach and application to determination of Co(II) in the ng ml^{-1} level and novel characterization of Co(II) and Zn(II) complexes with 1,5-di(2-hydroxy-5-sulfophenyl)-3-cyanoformazan

Hong-Wen Gao,*[ab] Hong-Yan Wang,[bc] Sheng-Yi Zhang[b] and Jian-Fu Zhao[a]

[a] *State Key Laboratory of Pollution Control and Resources Reuse, School of Environmental Science and Engineering, Tongji University, Shanghai 200092, P. R. China. E-mail: hwgao@mail.tongji.edu.cn*
[b] *Department of Chemistry, Anhui University, Hefei 230039, P. R. China*
[c] *Department of Chemistry and Biology, Suzhou Teachers College, Suzhou 234000, P. R. China*

Received (in Montpellier, France) 15th June 2003, Accepted 19th August 2003
First published as an Advance Article on the web 7th October 2003

The light-absorption ratio variation approach (LARVA) has been established and applied to the determination of Co on the ng ml^{-1} level with 1, 5-di(2-hydroxy-5-sulfophenyl)-3-cyanoformazan (DSPCF) at pH 9.33. Competitive replacement complexation (CRC) among DSPCF, Zn(II) and Co(II) as described was used to improve the analytical selectivity. The determination of the complex formation constants was also improved. Results have shown that ΔA_r^{-1} (where ΔA_r is the light-absorption ratio variation) is linear in the range of Co(II) between 10 and 200 ng ml^{-1}. The limit of detection (3δ) of Co(II) is only 3.7 ng ml^{-1}. The combination of CRC and LARVA has been applied to the analysis of water quality with satisfactory results.

Introduction

In trace analysis, especially in control of materials and the environmental, a number of expensive instruments such as ICP-AES, ETAAS and XRF are used extensively. Most of them are used for elemental analysis and often offer a high sensitivity and carry out the simultaneous determination of multiple components. However, they are not appropriate for the study of the mechanism of a chemical reaction and for molecular morphological analysis. From the periodic reviews of "ultraviolet and light absorption spectrometry" published from 1978 to 1998,[1] we learn that spectrophotometry is an effective and practical analytical method though its study trends to weaken in recent years, particularly in advanced countries. The development of reagents, analytically significant chromophoric systems and spectrophotometric methodology provides light absorption spectrometry with a very wide range of applications for the analysis of food,[2] water quality[3] and tropospheric substances[4] and in the identification of gems,[5] studies of inorganic particle formation,[6] solid-phase structures[7] and protein folding and unfolding.[8] Nowadays, activity in the area of spectrophotometric analysis of inorganic species seems to have remained relatively constant. In the area of photometric methods for organic substances, activity has not significantly increased but continues to center around applications in the clinical, pharmaceutical and biological areas. Many of the improvements including instrumentation and components,[9] chemometrics[10] and optimization techniques[11] have been significantly developed. Computers and microprocessors seem to be stimulating a great deal of interest in the areas of multiple wavelength,[12] derivative[13] and flow injection techniques.[14] All of these have played an important role in the improvement of selectivity, accuracy, sensitivity and precision of trace analysis.

The addition of an assistant such as a surfactant,[15] a cyclodextrin[16] or an association ion[17] is often necessary in a color reaction, too. For the same purposes as above, many highly sensitive chromophores such as porphyrins, hydrazine and its derivatives, oximes and sulfonates are increasingly synthesized and applied.[18] In spite of these efforts, the sensitivity up-limit of spectrophotometric analysis has not yet been substantively improved.

In the present work, the light-absorption ratio variation approach (LARVA) is proposed. It is established on the basis that a sensitive variation of the light-absorption ratio of a reaction between a chromophore and a detected component appears with the component concentration at the ultra-trace level. In order to enhance selectivity of the reaction, a conventional method is to add a number of masking reagents in the solution. However, competitive replacement complexation (CRC)[19] is simple and effectively improves the selectivity; it is described and applied in the present work. The spectral correction technique (SCT)[20] is a very useful method for the characterization of a chemical reaction such as ligand-metal complexation or the interaction between small molecules and biomacromolecules.[21] The combination of SCT, CRC and LARVA not only characterizes clearly the complexation but also make trace analysis much more selective and highly sensitive.

In the present work, 1,5-di(2-hydroxyl-5-sulfophenyl-)-3-cyanoformazan (DSPCF) was selected as the ligand to complex Co(II) and Zn(II) at pH 9.33. DSPCF is a strong colorant with a high molar light absorptivity ($\varepsilon_{548nm} = 1.47 \times 10^4$ l mol^{-1} cm^{-1}). Its structure, shown in Fig. 1, belongs to the cyanoformazan group and is a typical multi-coordinative ligand. It may complex many metal ions such as Cu(II), Fe(II), Zn(II), Mn(II), Ni(II), Co(II), Al(III) and Pb(II) to form binary complexes. So, it is not fit for the direct determination of any individual metal ion. However, we found that Co(II) may replace the Zn(II) coordinated in the Zn-DSPCF complex to form a blue Co-DSPCF complex. The replacement complexation is sensitive and selective in the presence of a high concentration

This journal is © The Royal Society of Chemistry and the Centre National de la Recherche Scientifique 2003

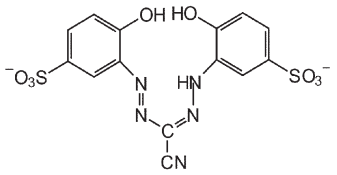

1,5-di(2-hydroxyl-5-sulfophenyl)-3- cyanoformazan (DSPCF)

Fig. 1 Chemical structure of DSPCFH.

of Zn(II). The Zn-DSPCF and Co-DSPCF complexes have been characterized by SCT and replacement complexation has been used for the determination of Co(II) at the ng ml^{-1} level in water by LARVA. Certainly, the Zn/Co-DSPCF reaction is only an example. In fact, many similar complexations such as metal ion-dye ligand, protein-organic molecule or drug-oxidant can be characterized by SCT and most of these might be used for the ultra-trace analysis of metal ions, drugs, biomacromolecules, inorganic and organic compounds by LARVA in the future.

Principles

Improvement in the determination of the stepwise stability constants K_n

In the earlier determinations of the stepwise stability constants (K_1, ..., K_n, ..., K_N) of a ligand (L)–metal (M) complex ML_N (where N is the maximum coordination number), several repetitive measurements of only a single solution were used.[19–21] Thus, it is possible for K_n to have an assignable error. Here, a multi-point measurement method was established and the accurate determination of K_n can be made by linear regression. The complexation between L and M (M_1 or M_2) illustrated in Fig. 2 proceeds *via* the stepwise reactions:

$$L + M \xrightleftharpoons{K_1} ML$$

$$L + ML \xrightleftharpoons{K_2} ML_2$$

$$\cdots\cdots\cdots\cdots$$

$$L + ML_{n-1} \xrightleftharpoons{K_n} ML_n$$

$$\cdots\cdots\cdots\cdots$$

$$L + ML_{N-1} \xrightleftharpoons{K_N} ML_N$$

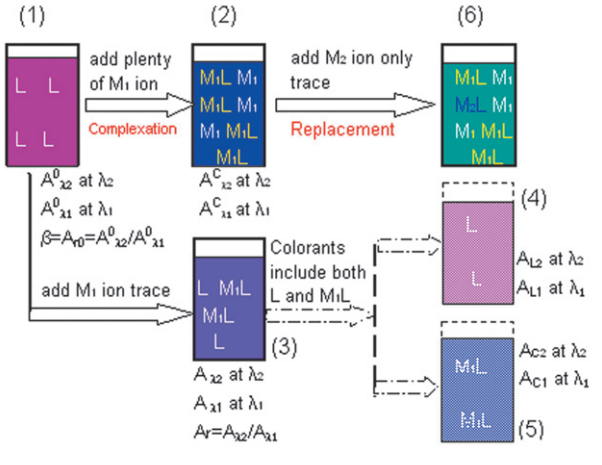

Fig. 2 Schematic of the color reaction between L, M_1 and M_2: (1) L solution (purplish red), (2) M_1L complex solution (blue) where $C_{M1} \gg C_{L0}$, (3) M_1–L reaction solution (violet) consisting of (4) an excess of L (light red) and (5) M_1L complex (light blue), (6) color mixture of M_1L (blue) and M_2L (green) where M_1 is replaced in a number of M_1L complexes by M_2 to form the M_2L complex.

The effective fraction (η) of L and the complexation ratio (γ) of L to M are determined and calculated by the relations:[20]

$$\eta = \frac{A_{C2} - A_{\lambda 2}}{A^0_{\lambda 2}} + 1 \quad (1)$$

and

$$\gamma = \eta \times \frac{C_{L0}}{C_{M0}} \quad (2)$$

where

$$A_{C2} = \frac{A_{\lambda 2} - \beta A_{\lambda 1}}{1 - \alpha\beta} \quad (3)$$

and where the symbols C_{M0} and C_{L0} are the initial concentrations of M and L. In Fig. 2(1), 2(3) and 2(5) and Fig. 3(A), A_{C2} indicates the real absorbance of only the ML complex at wavelength $\lambda_2$against water, which cannot be measured directly. $A^0_{\lambda 2}$ is the absorbance of the L solution measured at λ_2 against water. The symbols $A_{\lambda 2}$ and $A_{\lambda 1}$ are the absorbances of the M–L solution, respectively measured at $\lambda_2$and λ_1 against water. Both β and α are correction constants and they may be calculated from curves 1 and 2 by means of:

$$\beta = \frac{A^0_{\lambda 2}}{A^0_{\lambda 1}} \quad (4)$$

and

$$\alpha = \frac{A^C_{\lambda 2}}{A^C_{\lambda 1}} \quad (5)$$

The M–L solution with a γ of L to M varying between $n-1$ and n mostly consists of both ML_{n-1} and ML_n complexes and free L, especially for $n - 0.7 < \gamma < n - 0.3$. Thus, the other complexes ML_{n-2} and ML_{n+1}only represent a too small fraction to affect the determination of K_n. The n-step stability constant (K_n) of complex ML_N is calculated by the relation:

$$y = K_n x \quad (6)$$

where

$$x = C_{L0} - \gamma C_{M0}$$

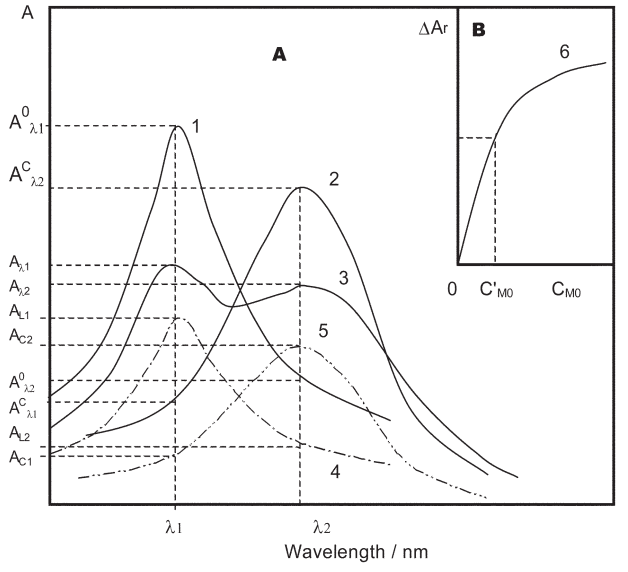

Fig. 3 (A) Plots of the absorption spectra for the establishment of the LARVA methodology: (curve 1) solution of L, (curve 2) ML complex solution without free L, (curve 3) M–L reaction solution, (curve 4) virtual spectrum of excess of L from curve 3 and (curve 5) virtual spectrum of ML complex formed from curve 3. B- Plots of ΔA_r *vs.* C_{M_0}.

and

$$y = \left(\frac{1}{n-\gamma} - 1\right)$$

(for $n - 0.7 < \gamma < n - 0.3$).

Therefore, each K_n can be determined by varying the molarity of L in a constant molarity M solution. From all K_n, the cumulative stability constant (K) of ML_N is calculated by:

$$K = \prod_{n=1}^{N} K_n \tag{7}$$

Eqn. (7) is now for the first time derived and applied in this work.

Light-absorption ratio variation approach

The stepwise complex reactions above are merged as follows:

	$n\,\mathbf{L}$	+	$\mathbf{M}$	$\rightleftharpoons$	$\mathbf{ML}_n$
Initiation	C_{L0}($A^0_{\lambda1}$ at λ_1 and $A^0_{\lambda2}$ at λ_2)		C_{M0}		0
Equilibrium	$C_L = C_{L0} - nC_{M0}$ (A_{L1} at λ_1 and A_{L2} at λ_2)		$C_M \to 0$		C_{M0}(A_{C1} at λ_1 and A_{C2} at λ_2)

From the illustration in Figs 2(1), 2(3), 2(4), 2(5) and 3(A),

$$A_{\lambda1} = A_{L1} + A_{C1} \tag{7}$$

and

$$A_{\lambda2} = A_{L2} + A_{C2}$$

$$A_r = \frac{A_{\lambda2}}{A_{\lambda1}} = \frac{A_{L2} + A_{C2}}{A_{L1} + A_{C1}} = \frac{\delta C_L \varepsilon^L_{\lambda2} + \delta C_{M0}\varepsilon^{ML}_{\lambda2}}{\delta C_L \varepsilon^L_{\lambda1} + \delta C_{M0}\varepsilon^{ML}_{\lambda1}},$$

$$A_{r0} = \frac{A^0_{\lambda2}}{A^0_{\lambda1}} = \frac{\delta C_{L0}\varepsilon^L_{\lambda2}}{\delta C_{L0}\varepsilon^L_{\lambda1}}$$

$$A_r - A_{r0} = \frac{C_L\varepsilon^L_{\lambda2} + C_{M0}\varepsilon^{ML}_{\lambda2}}{C_L\varepsilon^L_{\lambda1} + C_{M0}\varepsilon^{ML}_{\lambda1}} - \frac{\varepsilon^L_{\lambda2}}{\varepsilon^L_{\lambda1}}$$

$$\Delta A_r = \frac{\left(\varepsilon^L_{\lambda1}\varepsilon^{ML}_{\lambda2} - \varepsilon^L_{\lambda2}\varepsilon^{ML}_{\lambda1}\right)C_{M0}}{\left(C_{L0} - nC_{M0}\right)\left(\varepsilon^L_{\lambda1}\right)^2 + C_{M0}\varepsilon^{ML}_{\lambda1}\varepsilon^L_{\lambda1}}$$

$$\Delta A_r^{-1} = \frac{C_{L0}\left(\varepsilon^L_{\lambda1}\right)^2}{\varepsilon^{ML}_{\lambda2}\varepsilon^L_{\lambda1} - \varepsilon^{ML}_{\lambda1}\varepsilon^L_{\lambda2}} \cdot C^{-1}_{M0} + \frac{\varepsilon^L_{\lambda1}\left(\varepsilon^{ML}_{\lambda1} - n\varepsilon^L_{\lambda1}\right)}{\varepsilon^{ML}_{\lambda2}\varepsilon^L_{\lambda1} - \varepsilon^{ML}_{\lambda1}\varepsilon^L_{\lambda2}}$$

$$\therefore \Delta A_r^{-1} = p' C^{-1}_{M0} + q' \tag{8}$$

where

$$p' = \frac{C_{L0}\left(\varepsilon^L_{\lambda1}\right)^2}{\varepsilon^{ML}_{\lambda2}\varepsilon^L_{\lambda1} - \varepsilon^{ML}_{\lambda1}\varepsilon^L_{\lambda2}}$$

and

$$q' = \frac{\varepsilon^L_{\lambda1}\left(\varepsilon^{ML}_{\lambda1} - n\varepsilon^L_{\lambda1}\right)}{\varepsilon^{ML}_{\lambda2}\varepsilon^L_{\lambda1} - \varepsilon^{ML}_{\lambda1}\varepsilon^L_{\lambda2}}.$$

Both p' and q' are constants.

A sketch of eqn. (8) is shown in Fig. 3(B). The plot ΔA_r *vs.* C_{M_0} is linear when the molarity of M is much less than that of L, that is C'_{M0}. Thus, eqn. (8) can be rewritten as:

$$\Delta A_r = pC_{M_0} + q \tag{9}$$

where the symbols p and q are constants. Eqns. (8) and (9) can both be directly used in quantitative detection of traces of M. This method is called the light-absorption ratio variation approach (LARVA). From the equation above, the sensitivity factor p'^{-1} is the inverse ratio of C_{L0}. Therefore, the analytical sensitivity increases as less L is added. Nevertheless, a too-low amount of L will certainly bring an obvious error—an increase in the contribution of the instrument's noise signal. Therefore, the higher the light absorptivity of the chromophore and the more sensitive the spectrometer, the lower the detection limit of a component in the LARVA method. In the present case, the addition of the chromophore to produce a peak absorbance between 0.05 and 0.2 is suggested.

Competitive replacement complexation (CRC)

In order to improve the analytical selectivity, CRC was developed and it has been applied to a number of complexation processes with satisfactory results.[19] As shown in Fig. 2(1) and 2(2), in the reaction between L and M_1, all of the L molecules are complexed by M_1 when the M_1 molarity is much higher than the L molarity. Thus, only one colored compound, the M_1L complex, exists in such a solution. However, the addition of M_2 will replace competitively M_1 from the M_1L complex to form a mixture of both the colored complexes M_1L and M_2L, as shown in Fig. 2(6). Thus, the M_1L complex is regarded as a new chromogenic reagent to use in the determination of trace amounts of M_2. Because M_1 is present in a high enough amount in the replacement reaction, only the M_1L (1 : 1) complex is formed and it will prevent the interference of many metal ions possibly present at the micro level in a sample. In most cases, it is not necessary to add any masking reagent in trace analysis. Moreover, CRC obviously improves the analytical selectivity. LARVA is still appropriate for the replacement complexation.

Experimental section

Apparatus and reagents

Absorption spectra were recorded on a TU1901 spectrophotometer (PGeneral, Beijing). The pH of the solution was measured with a Model delta 320 pH-meter (Mettler Toledo Group, Shanghai). A Model BS110S electronic balance (Sartorius Instruments, Beijing) was used to accurately weight the standard substances and DSPCF. A Model 110R electric thermal constant-temperature bath was used to adjust the temperature of the replacement reaction. A Model PLA-SPEC ICP-AES (Leeman Instruments) was used to examine the quantitative result of Co(II) obtained by LARVA.

Stock standard solutions of Zn(II) (200 μg ml^{-1}) and Co(II) (200 μg ml^{-1}) were prepared by dissolving the metals in spectrometric purity in 20% hydrogen chloride and diluting with deionized water. Standard solutions of 1.00 μg ml^{-1} Zn(II), 0.100 and 1.00 μg ml^{-1} Co(II) were prepared daily by diluting the above stock solution. Standard stock DSPCF (0.800 mmol l^{-1}) solution was prepared by dissolving 243 mg of disodium 1,5-di(2-hydroxy-5-sulfophenyl)-3-cyanoformazan (content 80%, provided by Changke Reagents Institute of Shanghai) in 500 ml deionized water. It was used to complex Co(II) and Zn(II). The 0.200 μmol ml^{-1} DSPCF solution was prepared accurately by diluting its standard stock solution. The ammonium buffer solutions at pH 7.26, 8.05, 8.52, 9.11, 9.33, 9.59, 9.85, 10.11 and 10.52 were prepared with ammonia water and ammonium chloride or ammonium acetate. The Zn–DSPCF complex (0.0400 mmol l^{-1}) solution was prepared by mixing 80 ml of 200 μg ml^{-1} Zn(II), 25 ml of pH 9.33 buffer solution and 25.0 ml of 0.200 mmol l^{-1} DSPCF, then diluting to 250 ml with deionized water. Trace amounts of Co(II) may replace Zn from the Zn–DSPCF complex.

General procedures

Characterization of the Zn–DSPCF and Co–DSPCF complexation reactions. Into ten 10 ml calibrated flasks were added 1.00 μg of Zn(II), 1 ml of pH 9.33 buffer solution and 0.0200 mmol l^{-1} DSPCF solution from 0.00 to 6.00 ml in steps of

0.50 ml. The mixture was diluted to 10 ml with deionized water and mixed thoroughly. After 10 min, the absorbances were measured at 638 and 510 nm against water and A_C, C_L, η and γ were calculated by eqn. 1 and 2. In the same way, into another ten 10 ml calibrated flasks were added 2.00 ml of 1.00 μg ml^{-1} Zn(II) and the other reagents were added as above. Finally, both N and K_n can be calculated by a linear regression of eqn. 6. Thus, the Zn–DSPCF complex was characterized. Similarly, we used Co(II) to replace Zn(II) and the above procedures were repeated. The absorbances were measured at 695 and 558 nm against the reagent blank. The Co–DSPCF complex was characterized as well.

Determination of ultra-micro amounts of Co(II) in water. A water sample (5.00 ml) was added into a 10 ml flask and 1 ml of pH 9.33 buffer solution and 2.00 ml of the 0.040 mmol l^{-1} Zn-DSPCF complex solution were added. The solution was diluted to 10 ml with deionized water. After 10 min, the absorbances were measured against water. In the meantime, a reagent blank without Co(II) was prepared and measured the same as that above. Thus, ΔA_r is calculated by the relation:

$$\Delta A_r = \frac{A_{679\text{nm}}}{A_{574\text{nm}}} - \frac{A^0_{679\text{nm}}}{A^0_{574\text{nm}}} \quad (10)$$

where $A_{679\ \text{nm}}$ and $A_{574\ \text{nm}}$ are the absorbances of the Co–Zn(DSPCF) solution measured at 679 and 574 nm against water. $A^0_{679\text{nm}}$ and $A^0_{574\text{nm}}$ are the absorbances of the solution without Co(II), respectively measured at 679 and 574 nm against water. From eqns. (8) or (9), C_{Co} in the sample was calculated.

Results and discussion

Variation of absorption spectra with pH

The absorption spectra of the Co–DSPCF and Zn–DSPCF solutions in various pH buffer mediums are shown in Fig. 4. From the 9 curves in Fig. 4(A), the complexation between Co and DSPCF is always sensitive when the pH is less than 9.59. In the same way, from Fig. 4(B), curve 5 shows the highest absorption peak. In a basic solution with pH over 10, the dehydrogenation of two –OH and the protonation of –NH– of DSPCF will occur simultaneously and the mixed ligand complexes of Zn(II) and Co(II), that is Zn(OH)(DSPCF) and Co(OH)(DSPCF), will also be possibly formed. Thus, the coordination of DSPCF with Zn(II) and Co(II) is weakened. We also found that the replacement complexation between Co(II) and Zn(DSPCF) became difficult in a strongly basic solution. If the solution has a pH less than 9, it is possible that the buffer capacity of the ammonium acetate is inadequate for a practical sample. Therefore, a pH 9.33 ammonium chloride–ammonia buffer solution was selected for this work. From curve 5 in Fig. 4(A), the peak is located at 695 nm and the valley at 558 nm. From curve 5 in Fig. 4(B), the peak is located at 638 nm and the valley at 510 nm. These four wavelengths were used for the characterization of the Co–DSPCF and Zn–DSPCF complexes.

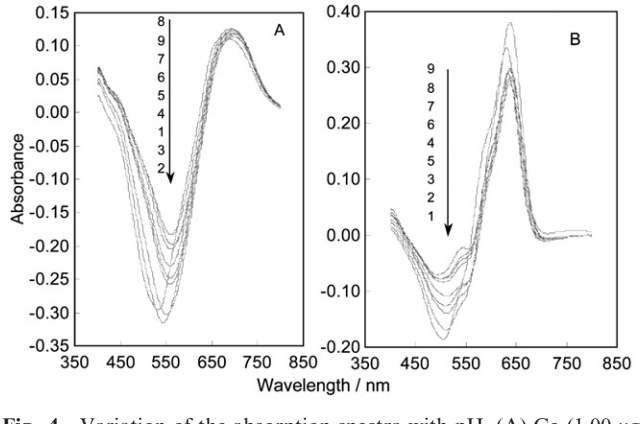

Fig. 4 Variation of the absorption spectra with pH. (A) Co (1.00 μg ml^{-1})–DSPCF (0.040 μmol ml^{-1}) solution measured against a blank without Co(II). (B) Zn (1.00 μg ml^{-1})–DSPCF (0.040 μmol ml^{-1}) solution measured against a blank without Zn(II). Spectra 1 to 9: pH 7.26, 8.05, 8.52, 9.11, 9.33, 9.59, 9.85, 10.11 and 10.52.

Composition of the complexes

From Fig. 5(A), the absorbance ratio $A_{558\ \text{nm}}/A_{695\ \text{nm}}$ of the Co–DSPCF solutions decreases rapidly with increase of Co(II) molarity. It approaches a minimum and remains constant when the amount of Co(II) is more than once that of DSPCF. This indicates that DSPCF is complexed almost completely with Co(II) and only a colored compound, the Co–DSPCF complex, exists in the presence of enough excess Co(II). The absorption spectrum of the Co–DSPCF complex is shown as curve 2 in Fig. 5(C). In addition, the break point approach[22] was applied to estimation of the complexation ratio. From Fig. 5(A) the break point is located at about a 0.5 : 1 ratio of Co to DSPCF. So the Co(DSPCF)$_2$ complex is possibly formed, which will be confirmed below. In the same way, from Fig. 5(B), the ratio $A_{510\ \text{nm}}/A_{638\ \text{nm}}$ of the Zn–DSPCF solutions approaches a minimum and remains constant when the amount of Zn(II) added is more than 0.8 times the DSPCF molarity. Only one colored compound, the Zn–DSPCF complex, exists in the presence of enough excess Zn(II) and its absorption spectrum is shown as curve 3 in Fig. 5(C). In addition, the break point in Fig. 5(B) is located at about a 0.35 : 1 ratio of Zn to DSPCF. So the Zn(DSPCF)$_3$ complex is possibly formed in this case. From Fig. 5(C), DSPCF is a violet solution at pH 9.33 and its peak absorbance is located at 548 nm with a molar light absorptivity of $\varepsilon = 1.47 \times 10^4$ l mol^{-1} cm^{-1} from curve 1 in Fig. 5(C). The Co–DSPCF complex is a green solution and its peak absorbance is located at 641 nm in curve 2. The Zn–DSPCF complex is a blue solution and its peak absorbance is located at 615 nm, as shown in curve 3. By comparing curve 1 with curves 2 and 3, the red shift of the peak of the Co–DSPCF complex reaches 93 nm but that of the Zn–DSPCF complex is only 67 nm. Therefore, the Co–DSPCF coordination bond is stronger than the Zn–DSPCF bond. From curves 1, 2 and 3, the correction coefficients were calculated to be $\beta^{\text{DSPCF}}_{638\text{nm}/510\text{nm}} = 0.451$, $\beta^{\text{DSPCF}}_{695\text{nm}/558\text{nm}} = 0.0667$, $\alpha^{\text{Zn(DSPCF)}}_{510\text{nm}/638\text{nm}} = 0.565$ and $\alpha^{\text{Co(DSPCF)}}_{558\text{nm}/695\text{nm}} = 0.616$. These will used to calculate η, γ and C_L below.

The variation of the γ value of DSPCF to Co(II) and Zn(II) with DSPCF molarity is shown in Fig. 6. γ approaches a maximum constant value of 2 in curve 1 and of 3 in curve 2 when DSPCF is more than 0.015 μmol l^{-1}. Therefore, the spectral correction technique confirms that complexes Co(DSPCF)$_2$ and Zn(DSPCF)$_3$ are formed at pH 9.33. The possible structures of ML complexes (1 : 1) are given in Fig. 7. The coordination of both Zn and DSPCF forms a macrocycle but its tightness is poor. The circle lengthens the conjugate chain consisting of the π-bond and lone pair electrons of oxygen and nitrogen to result in the spectral red shift of the Zn–DSPCF complex. However, because Zn is not coordinated directly with the –N=N–C(CN)=N–NH– functional group, the spectral red shift of the Zn–DSPCF complex is only 67 nm as mentioned above. Thus, the complexed Zn is easily replaced by other metal ions, for example Co(II). On the contrary, the O–Co–N chains divide the initial structure of the Co–DSPCF complex into three small adjacent circles so as to stabilize the complex structure. In addition, Co(II) coordinates directly to the head-N and the end-N of the –N=N–C(CN)=N–NH– functional group to dispersively extend its conjugation and this

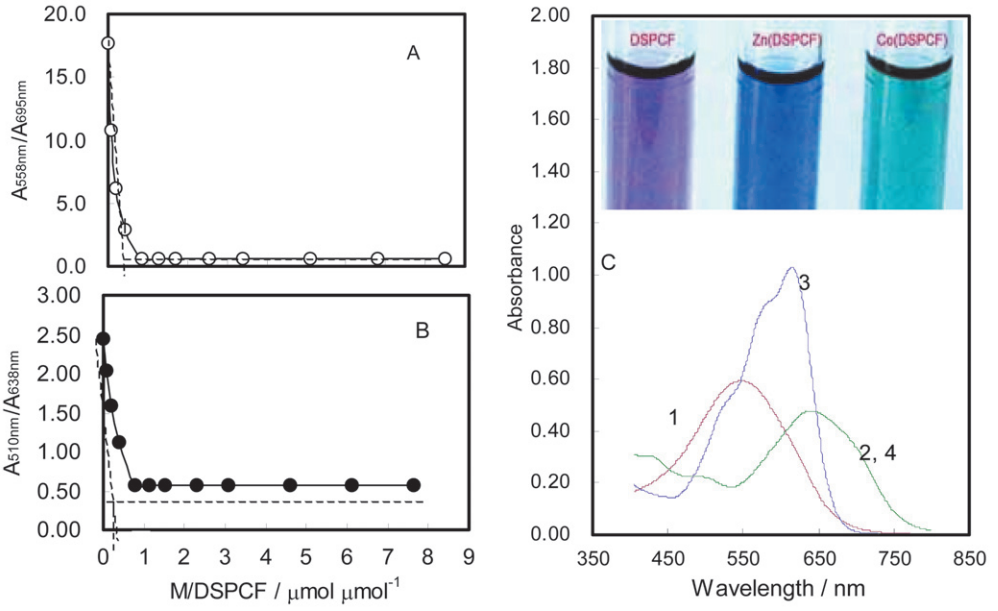

Fig. 5 Formation of the Co–DSPCF and Zn–DSPCF complexes at pH 9.33 where both the solutions no longer contain an excess of DSPCF . (A) Variation of $A_{558\ \mathrm{nm}}/A_{695\ \mathrm{nm}}$ *versus* the initial molar ratio of Co(II) to DSPCF (fixed at 0.040 μmol ml^{-1}). (B) Variation of $A_{510\ \mathrm{nm}}/A_{638\ \mathrm{nm}}$ *versus* the initial molar ratio of Zn(II) to DSPCF (fixed at 0.040 μmol ml^{-1}). (C) Curves 1, 2 and 3 are the absorption spectra of DSPCF, Co(DSPCF) and Zn(DSPCF) complexes, all at 0.040 μmol ml^{-1} measured against water, while curve 4 shows the absorption spectrum of the solution initially containing 0.040 μmol ml^{-1} Zn(DSPCF) and 0.1 μmol ml^{-1} Co(II) against water. The solutions' real color reactions are shown in the text tubes.

results in an obvious red shift of the absorption spectrum of the Co–DSPCF complex mentioned above.

Plots of $[(n-\gamma)^{-1}-1]$ *vs.* $(C_{L0}-\gamma C_{M0})$ of the solutions above are shown in Fig. 8. From curves 1 and 2 in Fig. 8(A), the first-step and second-step stabilities of complex $Co(DSPCF)_2$ were calculated to be $K_1 = 1.29\times10^7$ and $K_2 = 5.54\times10^5$ l mol^{-1}. With the same method, from curves 1, 2 and 3 in Fig. 8(B), the first-, second- and third-step stabilities of complex $Zn(DSPCF)_3$ were calculated to be $K_1 = 4.44\times10^7$, $K_2 = 5.56\times10^6$ and $K_3 = 1.22\times10^6$ l mol^{-1}. Thus, their cumulative stability constants are $K_{\mathrm{Co-DSPCF}} = 7.15\times10^{12}$ l^2 mol^{-2} and $K_{\mathrm{Zn-DSPCF}} = 3.01\times10^{20}$ l^3 mol^{-3}.

Competitive replacement complexation between Zn(DSPCF) and Co(II)

Analysis of the absorption spectra of the replacement complexation. From curves 2 and 4 in Fig. 5(C), we observe that two spectra are completely coincident. This means that the two solutions both contain only one identical colored complex, Co(DSPCF). Therefore, Co(II) replaces all Zn(II) in the Zn-(DSPCF) complex in the solution containing sufficient Co(II) at pH 9.33. However, from the results above, $K_{1,\mathrm{Co-DSPCF}} < K_{1,\mathrm{Zn-DSPCF}}$. Therefore, using only the difference in K_1 of two complexes to judge a replacement reaction is one-sided and sometimes even incorrect. In addition, the dynamics of the reaction and the stability of the chelated structure should also be considered.

Fig. 9 shows the absorption spectrum of the replacement complexation between Co(II) and Zn(DSPCF) complex at pH 9.33, measured against a reagent blank without Co(II). From the obvious peak–valley difference of the solution only containing 0.100 μg ml^{-1} Co(II), the replacement complexation

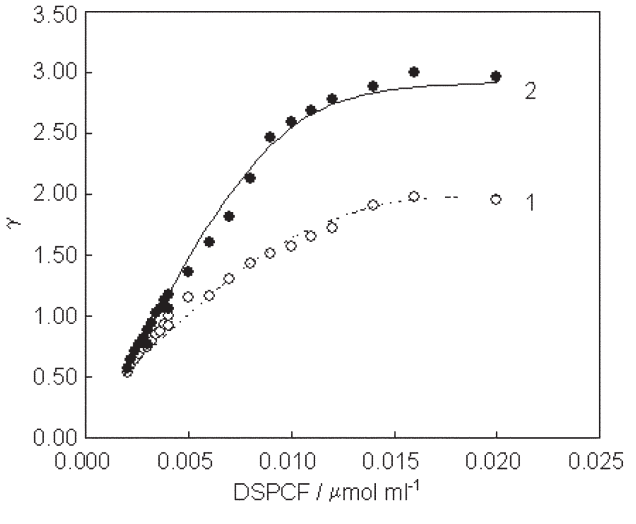

Fig. 6 Variation of γ with DSPCF molarity: curve 1 for Co and curve 2 for Zn (both at 0.200 μg ml^{-1}).

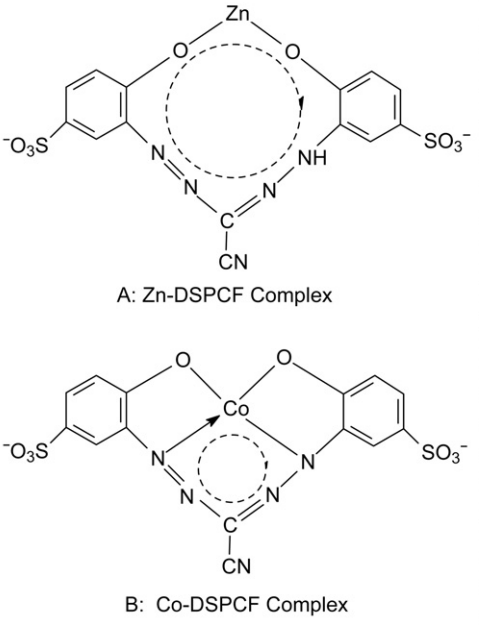

Fig. 7 Structural graphs of the Co–(DSPCF) and Zn–(DSPCF) complexes.

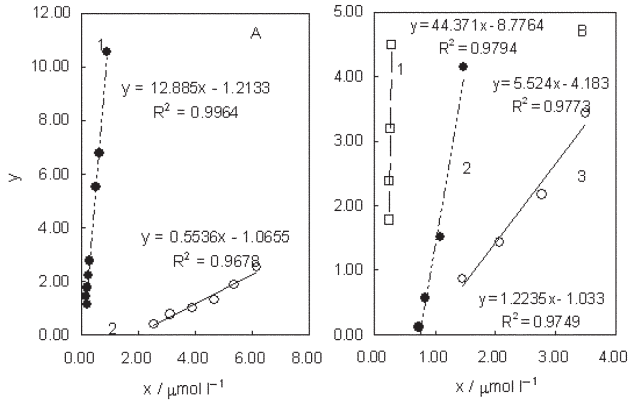

Fig. 8 Determination of the stepwise stability constants at pH 9.33 and 20 °C through plots of $[(n-\gamma)^{-1}-1]$ *vs.* $(C_{L0}-\gamma C_{M0})$. (A) Co–DSPCF complex and (B) Zn–DSPCF complex. Curve 1 is for the first-step stability constant (K_1), curve 2 for the second-step stability constant (K_2) and curve 3 for the third-step stability constant (K_3).

is very sensitive. The peak is located at 679 nm and the valley at 574 nm. These two wavelengths were used in the determination of ΔA_r below.

Effect of temperature and time on the replacement complexation. From curve A in Fig. 10, ΔA_r has a wave-like variation between 0.19 and 0.23 with temperature between 20 and 80 °C but the peak-valley difference occupies only about 20%. Therefore, 20 °C was selected for the replacement complexation. From curve B, ΔA_r reaches a maximum constant value after 20 min. The replacement reaction is rapid though the Zn(II) molarity is much greater than that of Co(II) in solution. The light absorption measurement of the replacement solution was thus carried out after coloring for 20 min.

Effect of the Zn–DSPCF complex on the replacement complexation. From the variations shown in Fig. 11 of ΔA_r of the solutions with a constant initial molar ratio of Co(II) to Zn(DSPCF) at 25 μg μmol^{-1}, ΔA_r decreases slowly with increasing Zn(DSPCF) concentration. The primary reason is that the self-aggregation of the Zn–DSPCF complex will not occur in dilute enough solution. In addition, the contribution of instrumental noise will increase, especially when the absorbance is less than 0.020. Of course, a high-sensitive and low-noise spectrometer can overcome such a defect. By comparing curves 1 and 2 in Fig. 11, one sees that the ΔA_r of the

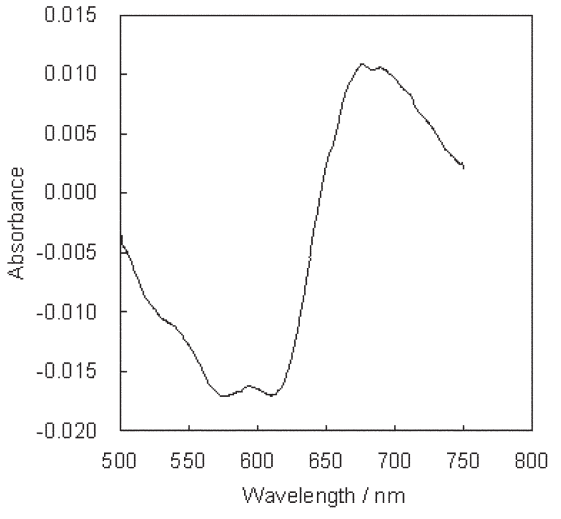

Fig. 9 Absorption spectrum of the replacement solution containing 0.0040 μmol ml^{-1} Zn(DSPCF) and 0.100 μg ml^{-1} Co(II), measured against a reagent blank without Co(II) at pH 9.33 and 20 °C.

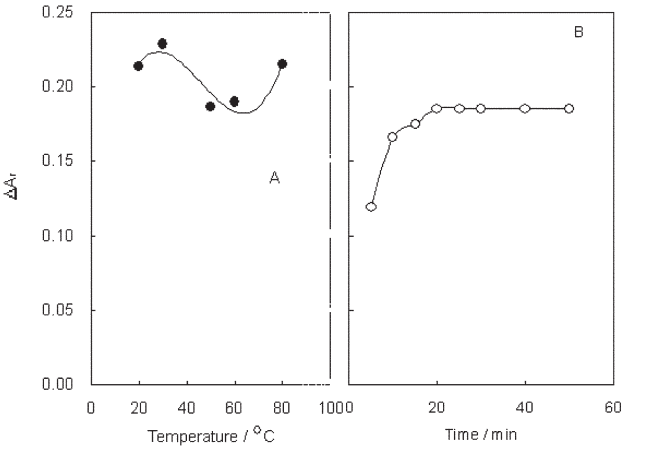

Fig. 10 Effect of temperature (A) and time (B) on ΔA_r of the replacement complexation reaction studied at 20 °C: (A) 0.0040 μmol ml^{-1} Zn(DSPCF) and 0.100 μg ml^{-1} Co(II), measured after coloring for 20 min; (B) 0.200 μg ml^{-1} Co(II) and 0.0080 μmol ml^{-1} Zn(DSPCF).

replacement complexation after coloring for 12 h is only 1.2 times higher than that after coloring for 0.5 h.

Calibration graphs and detection limit of Co(II)

Three series of standard Co(II) solutions between 0 and 0.200, 0 and 0.200 and 0 and 0.400 μg ml^{-1} were prepared and 1.00, 2.00 and 3.00 ml of 0.0400 mmol l^{-1} Zn(DSPCF) complex were added, respectively. The absorbances of each were measured. The ΔA_r of each solution was measured. The calibration graphs are shown in Fig. 12 and the parameters p' and q' of the regression equation $\Delta A_r^{-1} = p' C_{Co(II)}^{-1} + q'$ are given in Table 1. Plots of ΔA_r^{-1} *vs.* C_{CO}^{-1} are all linear. The detection limits of Co(II), defined as the blank value plus 3 times the standard deviation of 8 replicated blanks, were calculated and are also given in Table 1. By comparing them, Line 2 shows the lowest detection limit at only 3.7 ng ml^{-1}. Therefore, the addition of 2.00 ml of a 0.040 mmol l^{-1} Zn(DSPCF) complex solution to the replacement reaction solution gave the best results for the sensitive determination of ultra-micro amounts of Co(II) in water samples.

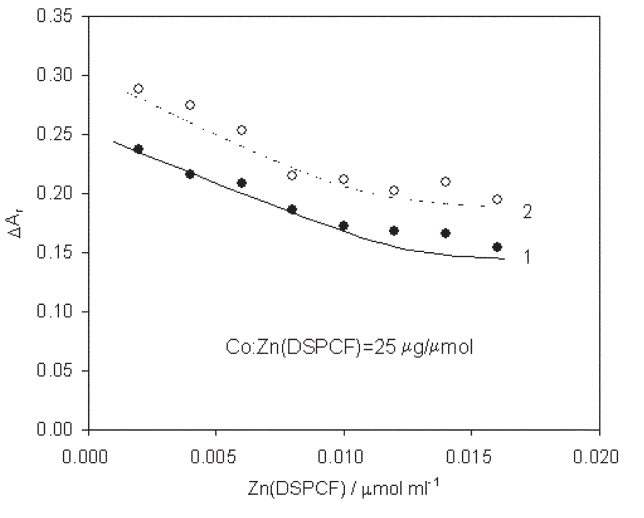

Fig. 11 Effect of Zn(DSPCF) concentration on ΔA_r of solutions initially containing DSPCF (from 0.0020 to 0.016 μmol ml^{-1}) and Co(II) (from 0.050 to 0.400 μg ml^{-1}), where the initial molar ratio of Co to Zn(DSPCF) always remain constant at 25 μg μmol^{-1}. Curve 1 measured 0.5 h after the beginning of the replacement reaction. Curve 2 measured after 12 h.

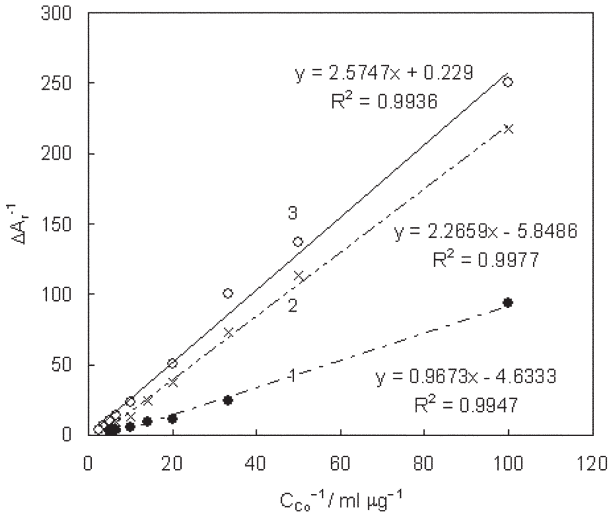

Fig. 12 Plots of ΔA_r^{-1} *vs.* C_{CO}^{-1} for the determination of Co(II) with Zn(DSPCF) complex as the replacement reactant at pH 9.33. Line 1: 0.0040 μmol ml^{-1} Zn(DSPCF) and Co(II) from 0.010 to 0.200 μg ml^{-1}; line 2: 0.0080 μmol ml^{-1} Zn(DSPCF) and Co(II) from 0.010 to 0.200 μg ml^{-1}; line 3: 0.0120 μmol ml^{-1} Zn(DSPCF) and Co(II) from 0.010 to 0.400 μg ml^{-1}.

Effect of foreign ions and compounds

In fact, DSPCF can coordinate many metal ions such as Pb(II), Cd(II), Hg(II), Al(II), Cu(II), Mn(II), Fe(II), Ni(II). However, we found that most metal ions, including Pb(II), Cd(II), Hg(II) and Al(II) in less than 10 mg l^{-1} levels will not complex DSPCF in the presence of plenty of Zn(II). Mn(II), Ni(II), Fe(II) and Cu(II) at the same concentration a Co(II) will not seriously affect the direct determination of Co(II). Simple organic compounds such as acetic acid, acetone, formal, ethanol, benzoic acid, lysine, cystine, glucose, citric acid, salicylic acid, tartaric acid, lactic acid and sodium dodecyl sulfate (SDS) at less than 10 mg l^{-1} levels did not interfere with the replacement coordination of Co(II). However, ethylenediamine tetraacetic acid (EDTA) and thiourea at over 3 mg l^{-1} levels will affect the direct determination of Co(II). The effects of sixteen metal ions and fifteen organic compounds on the replacement complexation are shown in Table 2. Beyond all doubt, the presence of a dye compound, for example, in a sample will interfere seriously with the absorption spectrum of the replacement complexation solution. Therefore, dye wastewaters must be pre-treated through an active carbon filter layer before coloring.

Analysis of water samples

As a test of the method, Co(II) in three water samples was determined. The results are listed in Table 3. The recovery rates of Co(II) added are between 90.1 and 104% and the RSD less than 11%. The samples were also examined, after pre-concentration of the samples, by inductively coupled plasma-atomic emission spectrometry (ICP-AES) and the results are also given in Table 3. The two methods show almost the same results. Therefore, LARVA is accurate and feasible for the ultra-trace analysis of a component.

Table 1 Standard regression equation parameters and detection limits for Co(II) obtained from Fig. 12

Line	Co(II)/ μg ml^{-1}	Zn(DSPCF) added/ mmol l^{-1}	p'	q'	R [a]	σ [b]	DT[c] /ng ml^{-1}
1	0–0.200	0.004	0.9673	−4.63	0.9973	0.00176	5.1
2	0–0.200	0.008	2.2659	−5.85	0.9988	0.00055	3.7
3	0–0.400	0.012	2.5747	0.229	0.9968	0.00068	5.3

[a] Linear correlation coefficient. [b] Standard deviation of 8 replicated blanks. [c] Detection limit of Co(II) was calculated by DT = $3\sigma p'$.

Table 2 Effect of foreign metal ions and organic compounds on the ΔA_r of a solution containing 2.00 μg of Co(II) and the error

Foreign ion or compound X	X added/ μg (10 ml)$^{-1}$	ΔA_r	% Error [a]
None	—	0.1630	0
Ca(II)	100	0.1561	−4.2
Mg(II)	50	0.1561	−4.2
Al(III)	10	0.1528	−6.2
Fe(II)	10	0.1599	−1.9
Fe(III)	10	0.1491	−8.5
Cu(II)	2.0	0.138	−15.4
Mn(II)	2.0	0.1621	+16.9
Pb(II)	10	0.1702	+4.4
Ni(II)	2.0	0.1854	+13.7
Cd(II)	10	0.1487	−8.8
Ge(IV)	5.0	0.156	−4.3
Sn(II)	10	0.1559	−4.4
Cr(III)	10	0.1584	−2.8
Ba(II)	10	0.1519	−6.8
V(V)	5.0	0.1444	−11.4
Hg(II)	5.0	0.1579	−3.1
Acetic acid	50	0.1561	−4.2
Acetone	20	0.1631	+0.1
Formal	20	0.1711	+5.0
Ethanol	50	0.1698	+4.2
Benzoic acid	10	0.1589	−2.5
Lysine	10	0.1671	+2.5
Cystine	10	0.1632	+0.1
Glucose	50	0.1786	+9.6
Citric acid	10	0.1681	+3.1
Salicylic acid	10	0.1743	+6.9
Tartaric acid	10	0.1519	−6.8
Lactic acid	10	0.1509	−7.4
EDTA	3	0.1501	−7.9
Thiourea	3	0.1517	−6.9
SDS	100	0.1619	−0.67

[a] Error = $(\Delta A_r^{X+Co} - \Delta A_r^{Co})/\Delta A_r^{Co} \times 100$

Conclusion

In principle LARVA is different from the traditional absorbance ratio[23], which is often used to examine the purity of an organic compound or to identify its structure, such as drugs,[23] polymers[24] or proteins.[25] It is suggested for LARVA to use a deeply colored chromophore and a low noise and highly sensitive spectrophotometer. Thus, it can play a

Table 3 Determination of Co(II) water samples

Sample from	Co(II) added/ mg l^{-1}	Co(II) found/ mg l^{-1}	% RSD	% Recovered
Mine well	0.000	< 0.0037 [a] (0.0025)[b]		
	0.050	0.048		96
Huaihe River	0.000	0.070 (±0.0019) [a] (0.075)[b]	2.66	
	0.100	0.160		90.1
Lake water	0.000	0.0041(±0.00045) [a] (0.0037)[b]	11	
	0.100	0.104		104

[a] Average of 3 replicate determinations. [b] One determination by ICP-AES after pre-concentration.

revolutionary role in trace analysis. Using this principle, many of the present color reactions may be improved notably. If applied to fluorophotometric analysis, the improvement of the sensitivity and selectivity should be obvious, too. The combination of SCT, CRC and LARVA is suitable for most of the color change reactions currently in use, including the quantitative detection of metal ions, inorganic and organic compounds, polymers and biomolecules in trace levels and analysis of the reaction mechanism occurring in diluted solutions, thin membranes and solid powders. Therefore, we believe that the originality of LARVA will strongly promote the design and synthesis of highly sensitive and selective chromophores.

References

1 (*a*) J. A. Howell and L. G. Hargis, *Anal. Chem.*, 1978, **50**, 243R; (*b*) J. A. Howell and L. G. Hargis, *Anal. Chem.*, 1982, **54**, 171R; (*c*) J. A. Howell and L. G. Hargis, *Anal. Chem.*, 1986, **58**, 108R; (*d*) J. A. Howell and L. G. Hargis, *Anal. Chem.*, 1990, **62**, 155R; (*e*) J. A. Howell and L. G. Hargis, *Anal. Chem.*, 1994, **66**, 445R; (*f*) L. G. Hargis and J. A. Howell, *Anal. Chem.*, 1980, **52**, 306R; (*g*) L. G. Hargis and J. A. Howell, *Anal. Chem.*, 1984, **56**, 225R; (*h*) L. G. Hargis and J. A. Howell, *Anal. Chem.*, 1988, **60**, 131R; (*i*) L. G. Hargis and J. A. Howell, *Anal. Chem.*, 1992, **64**, 66R; (*j*) L. G. Hargis, J. A. Howell and R. E. Sutton, *Anal. Chem.*, 1996, **68**, 169R; (*k*) J. A. Howell and R. E. Sutton, *Anal. Chem.*, 1998, **70**, 107R.

2 W. J. Hurst, in *Spectroscopy Techniques in Food Analysis*, ed. R. H. Wilson, VCH, New York, 1994, pp. 221–240.

3 O. Thomas, F. Theraulaz, C. Agnel and S. Suryani, *Trib. Eau*, 1995, **48**, 47.

4 U. Platt, *Eur. Comm., [Rep.] EUR*, 1994, **EUR 15609**, 664–673.

5 E. Fritsch, *Analusis*, 1995, **23**, M37.

6 A. Muramatsu, H. Itoh and T. Sugimoto, *Tohoku Daigaku Sozai Kogaku Kenkyusho Iho*, 1993, **49**, 101.

7 S. Matsuoka and K. J. Yoshimura, *Flow Injection Anal.*, 1995, **12**, 8.

8 H. Mach, D. B. Volkin, C. J. Burke and C. R. Middaugh, *Methods Mol. Biol. (Totowa, N.J.)*, 1995, **40**, 91.

9 (*a*) L. Ayllon, M. Silva and D. Perez Bendito, *J. Pharm. Sci.*, 1994, **83**, 1135; (*b*) I. E. Bechmann, L. Norgaard and C. Ridder, *Anal. Chim. Acta*, 1995, **304**, 229; (*c*) L. Norgaard and C. Ridder, *Chemom. Intell. Lab. Syst.*, 1994, **23**, 107; (*d*) O. Lee, A. P. Wade and G. A. Dumont, *Anal. Chem.*, 1994, **66**, 4507; (*e*) H. Liu and P. K. Dasgupta, *Anal. Chim. Acta*, 1994, **289**, 347; (*f*) R. Xiong, A. Velasco, M. Silva and D. Perez-Bendito, *Anal. Chim. Acta*, 1991, **251**, 313; (*g*) T. Umemura, Y. Kasuya, T. Odake and K. Tsunoda, *Analyst*, 2002, **127**, 149; (*h*) Y. Hirata and S. Katoh, *J. Microcolumn Sep.*, 1993, **4**, 503; (*i*) V. K. Popov, J. A. Banister, V. N. Bagratashvii, S. M. Howdle and M. J. Poliakoff, *Supercrit. Fluids*, 1994, **7**, 69.

10 (*a*) R. G. Brereton, *Analyst*, 1995, **120**, 2313; (*b*) H. Mark and J. Workman, *Spectroscopy (Eugene, Oreg.)*, 1994, **9**, 26; (*c*) H. Mark and J. Workman, *Spectroscopy (Eugene, Oreg.)*, 1994, **9**, 30; (*d*) D. Perez-Bendito, *Analyst*, 1990, **115**, 748; (*e*) A. Lorben, *Anal. Chem.*, 1984, **56**, 1004.

11 (*a*) W. Cao, F. Yongjian and Z. Shifu, *Fenxi Huaxue*, 1994, **22**, 781; (*b*) L. Costadinnova and T. Nedeltcheva, *Analyst*, 1995, **120**, 2217; (*c*) J. Zolgharnein, H. Abdollahi, D. Jaefarifar and G. H. Azimi, *Talanta*, 2002, **57**, 1067; (*d*) K. Mutaftchiev and K. Tzachev, *Phytochem. Anal.*, 2003, **14**, 160; (*e*) M. Bos and E. Hoogendam, *Anal. Chim. Acta*, 1992, **267**, 73.

12 (*a*) F. Bosch-Reig, A. Campins-Falcop, A. Sevillano-Cabeza, R. Herraez-Hernandez and C. Molins-Legua, *Anal. Chem.*, 1991, **63**, 2424; (*b*) V. Ulvi, *J. Pharm. Biomed. Anal.*, 1998, **17**, 77; (*c*) H. W. Gao, Y. C. Li, P. F. Zhang, M. Tao and L. Wang, *J. Anal. Chem.*, 2001, **56**, 1007.

13 (*a*) K. Kitamura, H. Mano, Y. Shimamoto, Y. Tadokoro, K. Tsuruta and S. Kitagawa, *Fresenius' J. Anal. Chem.*, 1997, **358**, 509; (*b*) M. Kazemipour, E. Noroozian, M. S. Tehrani and M. Mahmoudian, *J. Pharm. Biomed. Anal.*, 2002, **30**, 1379; (*c*) F. Salinas, J. B. Nevado and A. E. Mansilla, *Talanta*, 1990, **37**, 347; (*d*) C. B. Ojeda, F. S. Rojas and J. M. C. Pavon, *Talanta*, 1995, **42**, 1195.

14 (*a*) F. R. P. Rocha, P. B. Martelli and B. F. Reis, *Talanta*, 2001, **55**, 861; (*b*) I. E. Bechmann, L. Norgaard and C. Ridder, *Anal. Chim. Acta*, 1995, **304**, 229; (*c*) A. F. Danet and M. Cheregi, *Rev. Chim. (Bucharest)*, 1994, **45**, 604.

15 Q. F. Hu, G. Y. Yang, Z. J. Huang and J. Y. Yin, *Talanta*, 2002, **58**, 467.

16 G. Granero, C. Garnero and M. Longhi, *J. Pharm. Biomed. Anal.*, 2002, **29**, 51.

17 A. S. Amin and Y. M. Issa, *Spectrochim. Acta, Part A*, 2003, **59**, 6630.

18 (*a*) Z. J. Li, J. M. Pan and J. Tang, *Anal. Chim. Acta*, 2001, **445**, 153; (*b*) H. M. Ma, U. Jarzak and W. Thiemann, *New J. Chem.*, 2001, **25**, 872; (*c*) M. Su, Y. Liu, H. Ma, Q. Ma, Z. Wang, J. Yang and M. Wang, *Chem. Commun.*, 2001, 960; (*d*) S. Inoue and M. Uto, *Bunseki*, 1993, **11**, 877.

19 (*a*) H. W. Gao, *J. AOAC Int.*, 2001, **84**, 532; (*b*) H. W. Gao and N. L. Hu, *J. Chin. Chem. Soc. (Taipei)*, 2003, **49**, 965; (*c*) H. W. Gao and J. F. Zhao, *Croat. Chem. Acta*, 2003, **76**, 1.

20 (*a*) H. W. Gao and P. F. Zhang, *Analyst*, 1994, **119**, 2109; (*b*) H. W. Gao, *Talanta*, 2000, **52**, 817; (*c*) H. W. Gao, J. X. Yang, Z. Z. Zhou and J. F. Zhao, *Phytochem. Anal.*, 2003, **14**, 91.

21 (*a*) H. W. Gao and J. F. Zhao, *Aust. J. Chem.*, 2002, **55**, 767; (*b*) H. W. Gao and H. D. Mei, *Macromol. Biosci.*, 2002, **2**, 280; (*c*) H. W. Gao, J. Jiang and L. Q. Yu, *Analyst*, 2001, **126**, 528; (*d*) H. W. Gao, J. X. Yang and J. Jiang, *Supramol. Chem.*, 2002, **14**, 315.

22 H. W. Gao, Z. J. Hu and J. F. Zhao, *Chem. Phys. Lett.*, 2003, **376**, 251.

23 (*a*) F. Z. Tamura, *Bunseki Kagaku*, 1967, **16**, 193; (*b*) J. X. Chen and M. J. Xin, *J. Pharm. Anal.*, 1991, **11**, 225.

24 G. C. Pandey, Ajay Kumar and R. K. Garg, *J. Appl. Polym. Sci.*, 2001, **82**, 2135.

25 J. B. Murphy and M. W. Kies, *Biochem. Biophys. Acta*, 1960, **45**, 382.